

Lateral Separation of Macromolecules and Polyelectrolytes in Microlithographic Arrays

Deniz Ertas*

Lyman Laboratory of Physics, Harvard University, Cambridge, Massachusetts 02138

(Received 20 June 1997)

A new approach to separation of a variety of microscopic and mesoscopic objects in dilute solution is presented. The approach takes advantage of unique properties of a specially designed separation device (sieve), which can be built using already developed microlithographic techniques. Because of the broken reflection symmetry in its design, the *direction* of motion of an object in the sieve varies as a function of its self-diffusion constant, causing separation transverse to its direction of motion. This gives the device some significant and unique advantages over existing fractionation methods based on centrifugation and electrophoresis. [S0031-9007(98)05340-X]

PACS numbers: 87.15.-v, 07.10.-h, 36.20.Ey, 82.45.+z

Separation of macromolecules such as proteins and DNA, as well as mesoscopic objects such as cells and latex spheres, according to size has many important technological applications, and an immense effort has gone into achieving efficient, well-controlled and high-resolution separation techniques [1–3]. Two of the main avenues that have been employed extensively are electrophoresis [2] and centrifugation [3]. These two methods are somewhat complementary since the former typically separates by charge density and the latter by mass density. In particular, virtually all electrophoretic techniques rely on an electrophoretic mobility μ_e that changes as a function of molecular weight M_w , or some other characteristic for which separation is desired, since the separation occurs along the same direction as the average motion. An initially polydisperse band separates into many bands containing objects of different sizes as they travel at different velocities $\mathbf{v}(M_w) = \mu_e(M_w)\mathbf{E}$ along the direction of the applied field \mathbf{E} . A major obstacle to the electrophoretic separation of large polyelectrolytes with constant charge density such as nucleic acids is the independence of their electrophoretic mobility to their molecular weight in solution. To achieve separation, the polyelectrolytes are typically placed in a gel medium, where steric interactions generate a size-dependent μ_e . Despite significant progress in refined gel electrophoresis techniques, large objects such as cells or subcellular structures are very difficult to separate due to the limited range of achievable pore sizes, and issues such as sample loading and recovery are especially problematic for fragile specimens [2].

In this paper, a novel approach to separation, which embodies the advantages of both free flow electrophoresis [4] and gel electrophoresis, and is made possible by microlithographic techniques recently introduced by Volk-muth and Austin [1], is presented. The general idea is to design a particular electrophoresis chamber (sieve) such that the electrophoretic mobility tensor is nondiagonal, i.e., the objects do not move along the direction of applied electric field \mathbf{E} . Furthermore, the direction of mo-

tion varies as a function of size, causing objects of different sizes to move along different directions. As a result, this sieve causes lateral separation as in free flow electrophoresis [4] without the complications involved in creating a uniform transverse laminar flow field. The sieve is reusable, and the approach enables continuous operation since the paths are separated spatially rather than temporally, making retrieval of separated products extremely easy. These properties potentially provide a significant advantage over traditional methods as an analytical tool for separation of macromolecules.

The geometry of the sieve is shown in Fig. 1. It consists of a rectangular array of “cells” of periodicity $x_0 \times y_0$ that have a narrow entrance at the top and two exits at the bottom, which connect to the next row of cells. DNA fragments, characterized by a Kuhn length $b \approx 120$ nm, and a contour length $L = Nb$, enter from the top and move down the cell subject to an electric field $\mathbf{E} = E\mathbf{e}_y$. The radius of gyration R_g and the self-diffusion constant D_G of a DNA fragment with N Kuhn segments are given by

$$R_g \approx bN^\nu, \quad (1)$$

$$D_G \approx D_0N^{-\alpha}, \quad (2)$$

where $\nu = 1/2$ is the swelling exponent, $D_0 \approx 8 \mu\text{m}^2/\text{s}$ is the diffusion constant for each Kuhn segment, and $\alpha = 1/2$ for the Zimm model [5], where hydrodynamic interactions are taken into account [6]. For the Rouse model [7] (free draining conditions), D_0 is of the same order of magnitude, but $\alpha = 1$. The electrophoretic mobility of the fragments is independent of size and given by [8]

$$\mu_e = \frac{\lambda}{\zeta}, \quad (3)$$

where $\lambda \approx 0.3e^-/\text{\AA}$ and $\zeta \approx 3\pi\eta \approx 9 \times 10^{-3} \text{ kg/m s}$ [1] are the effective charge and friction coefficient per length of the DNA, respectively. (The Reynolds number is very small in all cases of interest, and inertial effects can be ignored.) For a DNA in this situation,

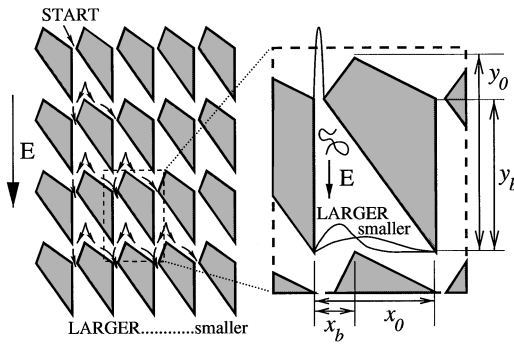


FIG. 1. The geometry of the sieve. Molecules enter the top of a cell from a narrow opening and diffuse away from the left wall as they are pulled down by the electric field. Smaller molecules diffuse farther and are therefore more likely to end up to the right of the branching point, located at a distance y_b from the entrance and x_b from the left wall. Therefore, the branching probability p_B , and subsequently the macroscopic mobility of a molecule, depends on its size.

$\mu_e \approx 5$ ($\mu\text{m/s}$)/(V/cm). Note that hydrodynamic interactions induced by Brownian motion are not screened by counterions, as is the case for electrophoretic velocity fields [9,10]. Consider a fragment that enters a cell at time t_0 and diffuses away from the left wall as it drifts down the cell. Ignoring its internal modes and characterizing its dynamics simply by its electrophoretic mobility μ_e and self-diffusion constant D_G , the probability of finding the DNA a distance x away from the left wall at time t when it has drifted a distance $y(t) = \mu_e E(t - t_0)$ from the top of the cell is given by

$$P_{\text{COM}}(x : y) \approx \frac{\mu_e E x}{2D_G y} \exp\left(-\frac{\mu_e E x^2}{4D_G y}\right), \quad (4)$$

which can be obtained from the solution to the diffusion equation with reflective (Dirichlet) boundary conditions on the left wall, and ignoring the effect of the right wall. A branching point is located at a distance x_b from the left wall and y_b from the top of the cell. Fragments that have diffused farther from the left wall than the branching point are funneled to the entrance of the cell diagonal to the original one, whereas those that are closer to the wall end up at the entrance to the cell immediately below. The probability of branching can be calculated from Eq. (4) as

$$p_B = \int_{x_b}^{\infty} dx P_{\text{COM}}(x : y_b) \approx \exp\left(-\frac{\mu_e E x_b^2}{4D_G y_b}\right). \quad (5)$$

For a DNA fragment of N segments,

$$p_B(N) \approx A e^{-(N/N_0)^\alpha}, \quad (6)$$

where

$$N_0 \approx \left(\frac{4D_0 y_b}{\mu_e E x_b^2}\right)^{1/\alpha} \quad (7)$$

is the characteristic separation size of the sieve, and A is a constant fitting parameter of $O(1)$. A remarkable observation is that N_0 can be tuned simply by changing the applied electric field, increasing the dynamic range of separation dramatically. For a reasonable feature size of $x_b \approx 1$ μm , $y_b \approx 4$ μm , varying the electric field in the range $E \approx 3$ – 25 V/cm, will yield characteristic separation sizes $N_0 \approx 70$ – 1 for the Zimm model, corresponding to DNA fragments of approximately 20000 and 300 base pairs, respectively.

Corrections to Eq. (6) involve internal relaxation of the polymer, full geometry of the cell, and diffusion along the field direction, among other effects. For example, the right wall can no longer be ignored for $N \approx \left(\frac{4D_0 y_b}{\mu_e E x_b^2}\right)^{1/\alpha} = N_0(x_b/x_0)^{1/\alpha} \approx N_0/16$ (for $x_0 \approx 4$ μm), and the finite size of the fragment becomes significant when $R_g \gtrsim x_b$, or equivalently $N \gtrsim (x_b/b)^{1/\nu} \approx 70$ for the parameters quoted above. Relaxation effects will be important when cell traversal time $y_b/(\mu_e E)$ is less than the principal relaxation time $0.325R_g^2/D_G$ [6], i.e., for $N > \left(\frac{D_0 y_b}{0.325\mu_e E b^2}\right)^{1/(\alpha+2\nu)} \approx 125$ for the more stringent situation of $E = 3$ V/cm. Analytical computation of these effects is beyond the scope of this paper, and in any case not very fruitful, since a numerically determined $p_B(N)$ (by simulating polymer dynamics with full boundary conditions, fluctuations, and internal relaxation modes) completely characterizes the separational properties of the sieve. The presented analysis is sufficient to obtain order-of-magnitude estimates of performance, which can be optimized by subsequent refinement based on such simulations.

In order to demonstrate the feasibility of such an approach, numerical integration of the equations of motion using the Rouse model for polymers [6,7] and reflecting boundary conditions at the walls has been performed, and is in reasonable agreement with analytical results. Figure 2 shows how the probability density for the center-of-mass (COM) position of a DNA fragment evolves as it moves down the cell. After the initial internal relaxation time, the probability can be fitted to the form of Eq. (5); the inset shows the expected linear increase in the mean square distance $\langle x^2 \rangle$ from the left wall as a function of distance y from the top of the cell. Figure 3 shows the branching probability $p_B(N)$ as a function of polymer size, and has the expected exponential behavior, even though the size of the polymers becomes quite large compared to the cell feature size. A correlation analysis of the time series of branching events confirms that they are statistically independent from one cell to the next.

At this point, it is useful to point out that any sieve design that breaks the left-right symmetry can, in principle, be used for purposes of separation. The underlying idea is

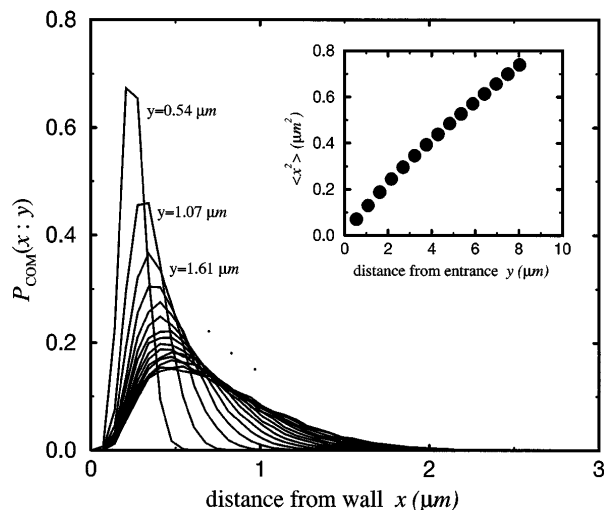


FIG. 2. Evolution of the density profile of DNA fragments with $N = 24$ Kuhn segments during the traversal of a cell. After an initial relaxation period, the profile takes approximately the form given by Eq. (5), and the mean square distance from the left wall increases linearly as a function of the distance from the entrance, as demonstrated in the inset. In this run, the primitive cell size of the rectangular lattice is $x_0 = 5 \mu\text{m} \times y_0 = 10 \mu\text{m}$; $y_b = 8 \mu\text{m}$ and $x_b = 0.64 \mu\text{m}$.

reminiscent of ratchet potentials [11], which have also been recently proposed as particle separators [12,13]. Both the ratchets and the sieve exploit differences in diffusion constants and steric constraints, and if the y axis is identified with time, the sieve can actually be thought of as the time history of a ratchet potential. However, unlike ratchets, the sieve does not require time-dependent potentials and is able to operate in a continuous mode.

Although this method of separation sounds very promising in principle, it is important to assess performance parameters and feasibility before a decision can be made about its practicality and whether it can compete against established techniques for certain tasks. One of the most important issues is the resolution that can be achieved [14]. A monodisperse packet of polymers

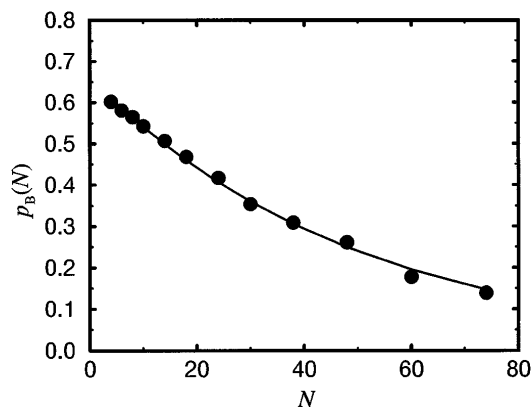


FIG. 3. Branching probability as a function of the number of segments N , for the cell parameters given in Fig. 2. The line is a fit to the exponential form (6) with $\alpha = 1$ and $N_0 \approx 50$.

with size N will spread laterally as it moves through the sieve, and after passing through M rows, the density profile of the band will exhibit a Bernoulli distribution whose peak is located at $X_P(M) = x_0 M p_B(N)$ and whose variance is $\sigma^2(N) = x_0^2 M p_B(N) [1 - p_B(N)]$ [15]. Hence, the full width at half-maximum (FWHM) of the corresponding band will be $\text{FWHM}(N) \approx 2x_0 \sqrt{2 \ln(2) p_B(N) [1 - p_B(N)] M}$. On the other hand, the peak separation between polymers of sizes N and $N + \delta N$ in a polydisperse sample will increase as $\delta X_P(N) = M x_0 (\delta N) [dp_B/dN]$. Thus, resolution can be improved indefinitely by passing the polymers through more rows of cells. Optimal resolution is achieved when $N \leq N_0$, for which $M \approx (4N/\delta N)^2$ rows are needed in order to resolve these two peaks. For a cell size of about $5 \mu\text{m}$, up to $M = 10^4$ rows should be feasible, enabling a resolution of about 4%. Note, however, that resolution can be further enhanced by gradient methods that are frequently implemented in gel electrophoresis [16], in this case by a spatially varying electric field or cell size. Fluctuations in $p_B(N)$ from cell-to-cell due to imperfections in the manufacturing of the sieve may further reduce the resolution; however, these tend to average out during the traversal of the sieve, and the additional variance due to these fluctuations will be smaller than the intrinsic variance $\sigma^2(N)$ by a factor $\delta p_B/p_B$, having a negligible impact on resolution provided that the sieve was built with reasonable tolerances. Even if there are significant systematic nonuniformities of the electric field (due to the dielectric properties of obstacles, etc.), they will not affect the resolution as long as the externally applied field is uniform, since the induced fields will be the same in each cell and will simply cause an overall shift in the branching probabilities. Another situation that may affect the resolution is the dependence of the DNA parameters on the specific base sequence. As long as the base sequences can be treated as random, the effect should be small compared to the intrinsic resolution, since there are about 300 base pairs in each Kuhn segment, which would cause a variation of less than 1%, reducing further with the number of segments as $N^{-1/2}$. Nevertheless, this effect might be important in situations where highly regular base pair sequences are involved. However, the impact on resolution in these cases can easily be assessed and taken into consideration, if necessary.

Another major concern is the throughput, which is affected by various factors, including cross-sectional area, concentration and velocity of the polymers, and ease of specimen loading and extraction. Original electrolithographic designs proposed and tested by Austin and co-workers were extremely shallow [1,17]. The sieve should be built as deep as possible to increase throughput. A stacked configuration might be considered if the mechanical stability of posts becomes a concern. A major bottleneck is the entrance to the sieve, since all polymers should start from the same point, rather than a band, to achieve

separation. This will cause much higher concentrations near the entrance to the sieve. (Actually, an initial spread comparable to the expected FWHM of the bands at the exit of the sieve will increase throughput without severely impacting the resolution.) Although a dilute solution is assumed in the calculation presented here, separation is not limited to the dilute regime and should occur in semidilute solutions as well, although the separation curve $p_B(N)$ is more difficult to compute. It can be determined without much difficulty by numerical simulation or experiments. The easy and quick extraction of the separated specimens enables continuous operation, in which polymers are constantly added at the entrance and extracted from exit channels placed at the bottom of the sieve. As a conservative estimate, let us consider DNA fragments of $1 \mu\text{m}$ in diameter ($N \approx 20$) moving at a velocity of $20 \mu\text{m/s}$. If the bottleneck at the entrance to the cell is about $1 \mu\text{m}$ and the cell depth is $10 \mu\text{m}$, and at the entrance the fragments are injected to 50 cells at a concentration in the dilute-semidilute boundary, a throughput of 10 000 fragments per sec, or 10 femtomoles per week, can be achieved. The travel time of a single fragment through a 5 cm sieve would be 40 min. Although expensive to produce, the sieves are tunable and reusable, significantly lowering their effective cost over their lifetimes. Thus, this technique may have major advantages over traditional methods as an analytical separation tool that can be easy to set up and automate, since no gel preparation or sample extraction is required.

The same technique can be applied to separation through centrifugation [3] as well. Individual sieves shaped as pie slices, with their entrances at the apex, can be arranged as stacked pies. The polydisperse solution can then be fed through a tube along the rotation axis, and separated objects can be collected in containers around the circumference that rotate with the sieves. Virtually any separation characteristic can be achieved by modulating the cell size as a function of distance to the rotation axis.

The particular design presented here is only one possibility and is by no means an optimal geometry, although its performance is expected to be quite satisfactory. On the other hand, the scalable structure of the sieve makes it possible to fully characterize device performance from a detailed modeling of dynamics within a single cell, significantly simplifying a numerical design effort. Furthermore, technological requirements for an experimental realization is well within today's capabilities, as has been demonstrated by Volkmuth *et al.* [1]. Therefore, experimental verification of the soundness of the general approach and a feasibility study of a prototype device is within reach in the very near future.

After completion of this work and initial submission for publication, I received communication from T. A. J.

Duke about ongoing independent work along very similar lines, which suggests that a prototype device based on the principles presented here is well underway [18]. I am grateful to him for informing me about their work, which provides an independent confirmation of the accuracy and feasibility of these ideas. A. Ajdari helped clarify certain issues related to electrophoresis of polyelectrolytes. This research was supported by the National Science Foundation, by the MRSEC program through Grant No. DMR-9400396, and through Grants No. DMR-9106237, No. DMR-9417047, and No. DMR-9416910.

*Present address: Exxon Research and Engineering, Clinton Township, Route 22 East, Annandale, New Jersey 08801. Electronic address: mdertas@erenj.com

- [1] W. D. Volkmuth and R. H. Austin, *Nature (London)* **358**, 600 (1992); W. D. Volkmuth *et al.*, *Phys. Rev. Lett.* **72**, 2117 (1994).
- [2] Ö. Gaál, G. A. Medgyesi, and L. Vereczkey, *Electrophoresis in the Separation of Biological Macromolecules* (Wiley, Chichester, 1980).
- [3] *Centrifugal Separations in Molecular and Cell Biology*, edited by G. D. Birnie and D. Rickwood (Butterworth & Co. Ltd., London, 1978).
- [4] K. Hannig, *Z. Anal. Chem.* **181**, 244 (1961).
- [5] B. H. Zimm, *J. Chem. Phys.* **24**, 269 (1956).
- [6] M. Doi and S. F. Edwards, *The Theory of Polymer Dynamics* (Oxford University Press, New York, 1986), pp. 91–103.
- [7] P. E. Rouse, *J. Chem. Phys.* **21**, 1272 (1953).
- [8] D. Long, J.-L. Viovy, and Armand Ajdari, *Phys. Rev. Lett.* **76**, 3858 (1996).
- [9] W. B. Russel, D. A. Saville, and W. R. Schowalter, *Colloidal Dispersions* (Cambridge University Press, Cambridge, UK, 1989), Chap. 7.
- [10] J. L. Barrat and J. F. Joanny, *Adv. Chem. Phys.* **94**, 1 (1996).
- [11] M. Magnasco, *Phys. Rev. Lett.* **71**, 1477 (1993).
- [12] A. Ajdari and J. Prost, *C. R. Acad. Sci. Paris* **315**, 1635 (1992).
- [13] G. W. Slater, H. L. Guo, and G. I. Nixon, *Phys. Rev. Lett.* **78**, 1170 (1997).
- [14] L. S. Lerman and D. Sinha, in *Electrophoresis of Large DNA Molecules—Theory and Applications*, edited by E. Lai and B. W. Birren (Cold Spring Harbor Laboratory Press, Plainview, New York, 1990), pp. 1–8.
- [15] S. Chandrasekhar, *Rev. Mod. Phys.* **15**, 1 (1943), Appendix I.
- [16] D. M. Hawcroft, *Electrophoresis* (Oxford University Press, New York, 1997), p. 26.
- [17] R. H. Austin *et al.*, U.S. Patent No. 5,427,663 (1995).
- [18] T. A. J. Duke and R. H. Austin, *Phys. Rev. Lett.* **80**, 1552 (1998).